

# Preparation and Characterization of Calcium Cross-linked Carboxymethyl Tamarind Kernel Polysaccharide as Release Retardant Polymer in Matrix

Vikas Dagar <sup>1</sup> , Rimpay Pahwa <sup>1</sup> , Munish Ahuja <sup>1,\*</sup> 

<sup>1</sup> Drug Delivery Research Laboratory, Department of Pharmaceutical Sciences, Guru Jambheshwar University of Science and Technology, Hisar 125001, India; vikas30dagar@gmail.com (V.D.), rimpypahwa28@gmail.com (R.P.); munishahuja17@yahoo.co.in (M.A.);

\* Correspondence: munishahuja17@yahoo.co.in (M.A.);

Scopus Author ID 7101943061

Received: 6.12.2021; Accepted: 6.01.2022; Published: 24.03.2022

**Abstract:** This study aims to improve the efficacy of carboxymethyl tamarind kernel polysaccharide by cross-linking with Ca<sup>2+</sup> ion and preparing its diclofenac sodium loaded matrix tablets for sustained drug delivery applications. Ionic gelation technique was used for cross-linking, and calcium chloride was used as a cross-linking agent. The native and cross-linked polysaccharide was characterized to analyze the change. The successful cross-linking of calcium was confirmed by infrared spectra by evaluating change in the functional group, while diffraction patterns revealed the change in crystallinity behavior. The thermal property of modified gum was also improved after Ca<sup>2+</sup> cross-linking, whereas microscopical images of both gums revealed the gum's change in shape and surface. Further, calcium cross-linked carboxymethyl tamarind kernel polysaccharide was formulated into a matrix tablet using diclofenac sodium. The weight variation, thickness, hardness, friability, content uniformity, moisture content, swelling index, and *in vitro* release kinetics were also evaluated. The *in vitro* release study revealed that modified gum tablets showed a sustained release of diclofenac sodium providing a release of 50.84 % of drug over 24 hours, following first-order kinetics with a super case – II transport mechanism. So, the results indicate that calcium cross-linking of CMTKP modifies its release behavior, making it suitable for preparing sustained release pharmaceutical formulation.

**Keywords:** carboxymethyl tamarind kernel polysaccharide; calcium cross-linking; ionic gelation; diclofenac sodium; sustained release.

© 2022 by the authors. This article is an open-access article distributed under the terms and conditions of the Creative Commons Attribution (CC BY) license (<https://creativecommons.org/licenses/by/4.0/>).

## 1. Introduction

Polysaccharides are non-biodegradable natural polymers that are gaining popularity as replacing synthetic polymers. The hybrid biomaterials created by combining biopolymers with inorganic materials have improved performance and increased the applications of biopolymers in the pharmaceutical, food, textiles, and paper industries [1,2]. Natural gums have been employed in pharmaceutical formulations as an antioxidant, binder, disintegrant, emulsifying agent, gelling agent, plasma expander, protective colloid, thickener, suspending agent, stabilizer, and as polymer matrices in tablets [3]. Guar gum, carrageenans, sodium alginate, gellan, locust bean, gum karaya, pectin, tragacanth, tamarind seed, katira, and other natural gum polysaccharides derived from plants have been extensively identified as excellent polymeric drug carriers for extended release over a prolonged period [4,5]. The key benefits

are biocompatibility, biodegradability, easy availability, and low cost of these natural polymers. However, their utility is hampered by unregulated hydration and microbial pollution, which can be upgraded physically or chemically by modifying them [6-8]. Various methodologies like carboxymethylation [3], cross-linking [9], grafting [10,11], thiolation [12], and others have been explored to meet customized determinations.

Tamarind kernel polysaccharide (TKP) is a natural branching polymer isolated from the endosperm of 'Indian date' (*Tamarindus indica* Linn.) of family *Leguminosae* [13,14]. TKP is made up of a  $\beta$ -D-glucan backbone chain, which is linked to side chains of  $\beta$ -D-galactopyranose and  $\alpha$ -D-xylopyranose. The ratio of glucose, xylose and galactose units is 2.80:2.25:1.00 [15]. It has a molecular mass of 720–880 kDa [16]. TKP is non-carcinogenic, biocompatible, and stable even at acidic pH levels [17,18]. So it can be employed in a variety of pharmaceutical formulations as a binder, thickening, emulsifier, suspending agent, and release modifier [19,20]. Carboxymethyl tamarind kernel polysaccharide (CMTKP) is obtained by carboxymethyl functionalization of TKP. It can be used over TKP because of TKP properties like dull color, an unpleasant odor, and low water solubility [21]. CMTKP is an anionic water-soluble derivative with stabilizing, gelling and release retardant properties [22]. The anionic character of CMTKP tends to interact with cationic moieties via the ionic gelation method [23]. The ionically gelled composite matrices formed by mixing CMTKP with anionic polymers like sodium alginate [24] and gelatin [25] have been used for controlled drug delivery and enzyme immobilization.

Calcium cross-linking over modified gum may result in a composite with specific controlled drug release properties. CMTKP is cross-linked with calcium to customize its properties in drug delivery applications by formulating matrix tablets with diclofenac sodium as the model drug. Diclofenac sodium, the model drug, was used in the study as it is the most frequently used non-steroidal anti-inflammatory drug for treating rheumatic and musculoskeletal disorders. It is highly effective with few side effects [26-28]. Earlier studies attempted to formulate diclofenac sodium formulations with a prolonged and controlled release to increase patient compliance [29,30]

In the current study, the physicochemical characterizations of CMTKP and calcium cross-linked CMTKP (C-CMTKP) gum were done by Fourier-transform infrared spectroscopy, differential scanning calorimetry, thermogravimetric analysis, X-ray diffraction, and field emission scanning electron microscopy-energy dispersive X-ray analysis. Further, the formulated matrix tablets were tested for thickness, hardness, friability, weight variation, content uniformity, moisture content, swelling index, and *in vitro* release kinetics of the drug.

## 2. Materials and Methods

### 2.1. Materials.

Carboxymethyl tamarind kernel polysaccharide (CMTKP) was procured as a gift sample from Hindustan Gums and Chemicals Ltd. (Bhiwani, India). Diclofenac sodium was gifted by Coax Bio-remedies Pvt. Ltd. (Hisar, India). Sodium hydroxide and calcium chloride were acquired from Sisco Research Laboratories Pvt. Ltd (Mumbai, India). Potassium dihydrogen orthophosphate anhydrous and Di-sodium hydrogen orthophosphate were purchased from High Purity Laboratory Chemicals Pvt. Ltd. (Mumbai, India).

## 2.2 Preparation of C-CMTKP from CMTKP.

Calcium cross-linking on CMTKP was done to enhance its functional properties for drug delivery applications. Initially, CMTKP was mixed with distilled water and sonicated in a bath sonicator (Powersonic 405, Hwashin Technology, Seoul, Korea) for 1h. The alkaline solution of sodium hydroxide (20ml, 1% w/v) was added into an aqueous solution of CMTKP (25ml, 5% w/v) for complete solubilization. Then, aqueous calcium chloride solution (30ml, 10% w/v) was added into the polymeric solution and stirred until precipitation occurred. The obtained precipitate was filtered, dried in a hot air oven (KI 137, Khera Instruments Pvt. Ltd., Mumbai, India) at  $50\pm 2^{\circ}\text{C}$  for 6 h, and stored in airtight container for further usage.

## 2.3. Characterization of CMTKP and C-CMTKP.

Characterization of CMTKP and C-CMTKP was done to detect the change in physicochemical properties of CMTKP after modification. The physical properties of powdered gum CMTKP and C-CMTKP were characterized by color, odor, bulk density, tapped density, and flow studies, including Carr's index, Hausner's ratio, and angle of repose by using standard protocols. The chemical properties were characterized by Fourier-transform infrared spectroscopy, differential scanning calorimetry, thermogravimetric analysis, X-ray diffraction, and field emission scanning electron microscopy – energy dispersive X-ray analysis.

### 2.3.1. Fourier-transform infrared spectroscopy (FT-IR).

FT-IR spectroscopy technique was used to determine the molecular composition of material and structure. The potassium bromide (KBr) disc method was used to record the infrared spectra of CMTKP and C-CMTKP. Small amounts of natural and modified gum with KBr were compressed into pellets individually using an IR hydraulic press (CAP-15 T, PCI Analytics, Mumbai, India). Using the FT-IR spectrophotometer (Spectrum BX, Perkin Elmer, UK), the IR spectra of CMTKP and C-CMTKP powdered gum were recorded in the range of  $4000\text{--}400\text{ cm}^{-1}$ .

### 2.3.2. Differential scanning calorimetry (DSC).

Differential scanning calorimetry (DSC 25, TA Instruments, USA) was used to determine the thermal properties of CMTKP and C-CMTKP powdered gum samples. Around 5 mg of powdered sample was airtightly fixed in an aluminum pan and screened between 10 to  $400^{\circ}\text{C}$  at a constant heating rate of  $10^{\circ}\text{C}/\text{min}$ . The melting temperature and enthalpy in the nitrogen atmosphere were recorded to complete the investigation.

### 2.3.3. Thermogravimetric analysis (TGA).

The thermal analysis measures sample weight loss or degradation as a function of temperature ( $^{\circ}\text{C}$ ). TGA was carried out using a thermal analyzer (Mettler-Toledo India Private Limited, Mumbai, India) to identify % weight loss as temperature increased over time. The standard alumina crucible was half-filled with a powdered gum sample. The crucible was inserted in the sample slot, and the analysis began at a temperature of  $10\text{--}400^{\circ}\text{C}$  at a rate of  $20^{\circ}\text{C}/\text{min}$ . The thermal curve was plotted for the evaluation of sample degradation characteristics.

#### 2.3.4. X-ray diffraction (XRD).

The XRD (Miniflex 600, Rigaku Corporation, Tokyo, Japan) technique was used to determine solid powder's crystalline or amorphous form. The diffraction pattern was recorded with a step size of  $0.02^{\circ}$  ( $2\theta$ ) in continuous scan mode. The diffractogram was documented using Ni filtered Cu  $K\alpha$  radiation at 30 kV operating voltages and 15 mA tube current with a scanning speed of  $2^{\circ}/\text{min}$ , between  $100$  to  $800^{\circ}$  ( $2\theta$ ).

#### 2.3.5 Field emission scanning electron microscopy-energy dispersive X-ray analysis (FESEM-EDX).

The FE-SEM (JSM-7610F Plus, JEOL, Japan) was used to detect the morphological characteristics of powdered gum samples of CMTKP and C-CMTKP. The sample was placed on a sample stub employing double-sided carbon adhesive tape. The gold coating was done for 40 seconds in the coating chamber (D II-29030SCTR, Smart coater, JEOL, USA) using the argon gas. Then micrographic images were captured at specific magnifications. EDX (EDAX, AMETEK -Materials Analysis Division, US) analysis was used to map the elements present in a powdered gum sample of CMTKP and C-CMTKP.

#### 2.4. Preparation of diclofenac-loaded matrix tablet.

The diclofenac sodium matrix tablets were prepared using CMTKP and C-CMTKP as described in the formula in Table 1. To prepare the matrix tablet, calcium di-phosphate as a binder, magnesium stearate as a lubricant, and diclofenac sodium as a model drug were mixed appropriately in CMTKP and C-CMTKP gum. In IR hydraulic press unit, the blended mixture was directly compressed into tablet form using biconvex punches and dies.

**Table 1.** Compositions of diclofenac-loaded matrix tablet.

Ingredients	Quantity (mg)	
	CMTKP	C-CMTKP
CMTKP	150	-
C-CMTKP	-	150
Diclofenac sodium	100	100
Calcium di-phosphate	150	150
Magnesium stearate	04	04

##### 2.4.1. Evaluation of tablet.

The weight variation, diameter, thickness, friability, hardness, content uniformity, moisture content, swelling index, and *in vitro* release of diclofenac sodium matrix tablets were all assessed.

##### 2.4.2. Weight variation.

Tablets from both batches of CMTKP and C-CMTKP were individually weighed in milligrams (mg) on an analytical balance (AY 220, Shimadzu, Japan). The average weight was determined, and the outcomes were expressed as mean  $\pm$  SD.

#### 2.4.3. Tablet thickness and diameter.

The thickness and diameter in millimeters (mm) of CMTKP and C-CMTKP tablets were measured using vernier caliper (YAMAYO® digital caliper, Japan). The thickness and diameter averages were reported, with the results expressed as mean ± SD.

#### 2.4.4. Hardness of tablet.

The tablet hardness tester (VTHT 500, VinSyst Digital Portable Tablet Hardness Tester, India) was used to determine the hardness of the tablet. The average was measured using CMTKP and C-CMTKP tablets that were selected at random. The result was given in Newton (N).

#### 2.4.5. Friability.

Six tablets were selected and weighed from both batches of CMTKP and C-CMTKP. In the Roche friabilator, each group of tablets was rotated at 25 rpm for 4 minutes (100 revolutions). The tablets were re-weighed to determine the weight difference after rotation. Equation 1 was then used to determine friability as % weight reduction from the initial tablets:

$$\% \text{ friability} = \frac{\text{Initial weight} - \text{final weight}}{\text{Initial weight}} \times 100 \quad (1)$$

#### 2.4.6. Moisture content.

Tablets were selected and weighed from both batches of CMTKP and C-CMTKP. Each tablet was placed in a hot air oven at 65°C and weighed at different time intervals. The procedure was repeated until the tablet's weight remained constant. Using equation 2, the percent moisture content was determined:

$$\% \text{ Moisture content} = \frac{\text{Initial weight} - \text{Final weight}}{\text{Initial weight}} \times 100 \quad (2)$$

#### 2.4.7. Drug content.

The actual amount of drug present in CMTKP and C-CMTKP tablets was determined by assessing the drug content. A specific quantity of weighed tablets was mixed with respective solvent, bath sonicated for 2h, and filtered using Whatman filter paper. The UV absorbance of the filtrate was measured at  $\lambda_{\text{max}}$  of 276nm to calculate the drug content in both tablets.

#### 2.4.8. Swelling study.

To assess the swelling index of both batches of CMTKP and C-CMTKP tablets, tablets were weighed and put in a beaker containing 25 ml of pH 6.8 and pH 1.2 phosphate buffer. The tablet was carefully removed at different time intervals, such as 5, 10, 15, 30, 60, and 120 minutes, wiped carefully, and weighed again. The procedure was halted when tablets began to dissolve or become overly dense. The swelling index was calculated using equation 3:

$$\% \text{ Swelling index} = \frac{\text{Final weight} - \text{Initial weight}}{\text{Initial weight}} \times 100 \quad (3)$$

2.4.9. *In vitro* dissolution study.

An *in vitro* drug release analysis was conducted using USP dissolution test type-II (iDisso-06, Electrolab Dissolution Tester, Mumbai, India) to evaluate the change in drug release behavior after modification of the official monograph of Extended-release tablet of diclofenac sodium. Tablets of market formulation of diclofenac sodium ‘Reactin<sup>®</sup>’, CMTKP and C-CMTKP were placed in a compartment of USP dissolution test apparatus containing release media (900 ml) with a pH of 1.2 for the first 2 h, followed by phosphate buffer with a pH of 6.8 for the next 24 h. The release media was maintained at 37°C temperature, and the paddle was rotated at 50 revolutions per minute. The aliquots (5ml) were withdrawn from the release media at different time points and performed by spectrophotometric assay (Genesys<sup>™</sup> 180, UV-Vis Spectrophotometer, ThermoFisher Scientific, USA) a maximum wavelength of 276 nm. The volume of the release media was compensated each time by adding the same volume of fresh buffer [31]. To find the best fitting model and understand the drug release mechanism, the cumulative percent drug release at different time points was plotted using the combined equations of various release kinetic models.

**3. Results and Discussion**

In this study, the interaction of CMTKP with Ca<sup>2+</sup> ions has been investigated for the preparation of matrix tablets. The Ca<sup>2+</sup> ion cross-linked CMTKP has been used as a release modifier in a tablet formulation for drug delivery applications. The procedure for the preparation of C-CMTKP from CMTKP is graphically represented in figure 1. The yield of modified gum (C-CMTKP) was found to be 37%. The color of CMTKP and cross-linked C-CMTKP gum was found to be light yellow and cream color, respectively. Both the gums were found to be odorless. Flow properties, including bulk density, tapped density, angle of repose, Hausner’s ratio, and Carr’s index, were determined in table 2. The results reveal that CMTKP shows passable flow, while C-CMTKP shows good flow properties. Further, both CMTKP and C-CMTKP gums were characterized employing FT-IR, DSC, TGA, XRD, and FESEM–EDX.

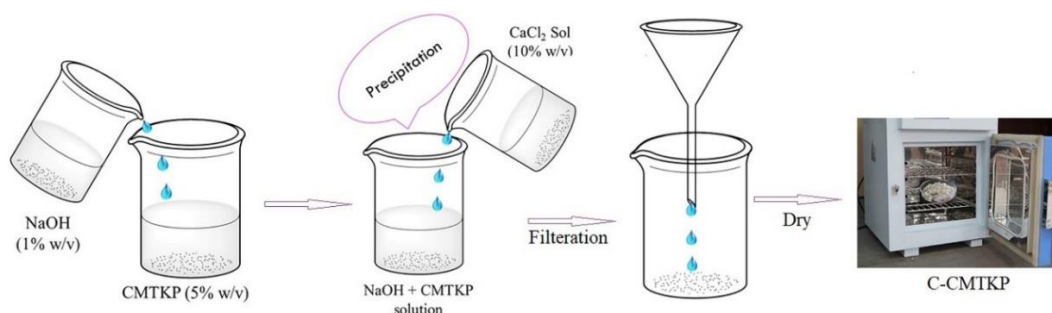
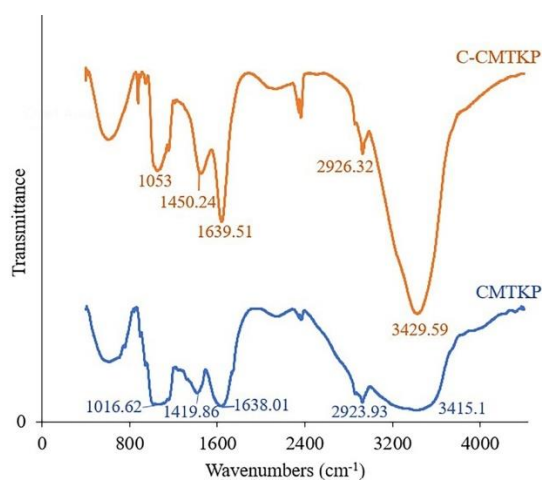


**Figure 1.** Graphical representation of the preparation of C-CMTKP from CMTKP.

**Table 2.** Pre-formulation evaluations of CMTKP and C-CMTKP.

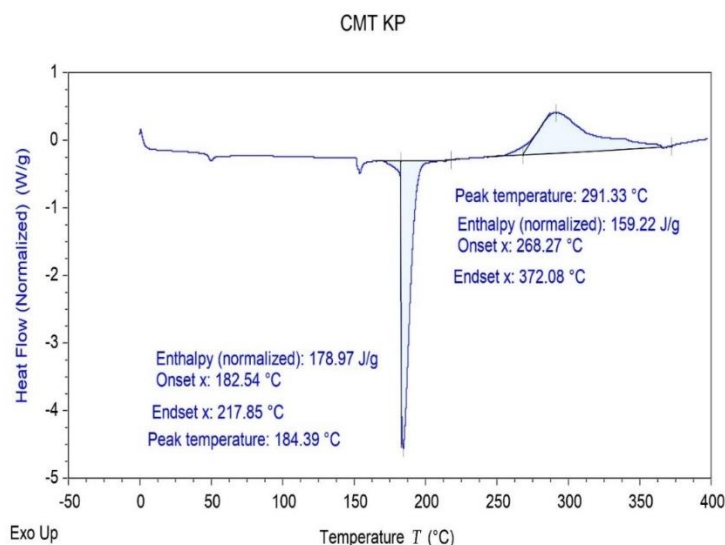
Parameters	CMTKP	C-CMTKP
Colour	Light yellow	Cream
Odour	Odourless	Odourless
Angle of repose (°)	45.53	34.60
Bulk density (g/ml)	0.4	0.71
Tapped density (g/ml)	0.52	0.83
Carr’s Index	23.07	14.45
Hausner’s ratio	1.30	1.16

Figure 2 shows the FT-IR spectra of CMTKP, displaying the absorption bands at  $3415.10\text{ cm}^{-1}$  and at  $2923.93\text{ cm}^{-1}$  due to -OH stretching and -CH stretching of the alkyl group, respectively. The peaks at  $1638.01\text{ cm}^{-1}$  and at  $1419.86\text{ cm}^{-1}$  can be assigned to C=O group of ester and -CH<sub>2</sub> bending vibrations, respectively while the peak at  $1016.62\text{ cm}^{-1}$  shows C-O-C stretching of ethers. On the other hand, FT-IR spectra of C-CMTKP display a narrow peak at  $3429.59\text{ cm}^{-1}$  due to the stretching of the hydroxyl group. The spectra show a peak at  $2926.32\text{ cm}^{-1}$  with an upfield shift attributed to the alkyl group's stretching. The peak at  $1639.51\text{ cm}^{-1}$  is attributed to the C = O group of the ester, the peak at  $1450.24\text{ cm}^{-1}$  is attributed to -CH<sub>2</sub> bending vibrations, and the peak at  $1053\text{ cm}^{-1}$  is attributed to C-O-C ether stretching. The peak of OH stretching in CMTKP is shifted from  $3415.10\text{ cm}^{-1}$  to  $3429.59\text{ cm}^{-1}$  due to interaction of the COOH group of CMTKP with Ca<sup>2+</sup> cations [32].

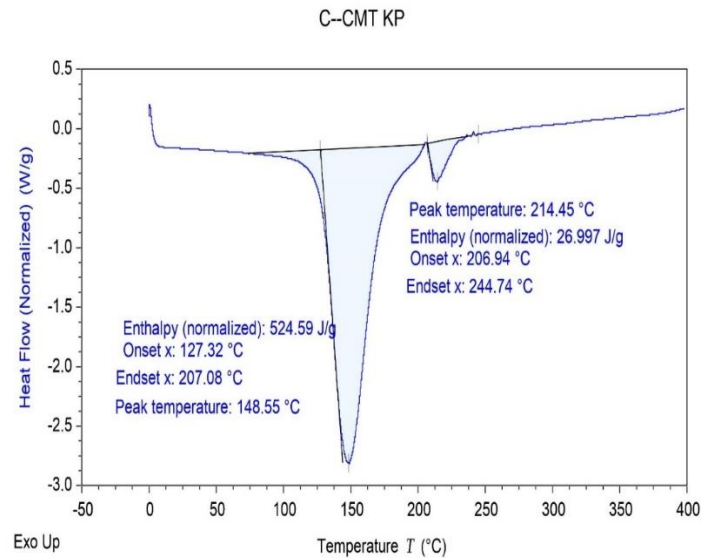


**Figure 2.** FT-IR Spectra of CMTKP and C-CMTKP.

Figure 3(a) and (b) shows the DSC thermogram of CMTKP and C-CMTKP, respectively. A broad endothermic peak followed by an exothermic peak was observed on the DSC thermogram of CMTKP. The endothermic peak was observed at  $184.39^\circ\text{C}$ , with an onset temperature of  $182.54^\circ\text{C}$  and a fusion enthalpy of  $178.97\text{ J/g}$ . The exothermic peak occurred at  $291.33^\circ\text{C}$ , with an onset temperature of  $268.27$  and a fusion enthalpy of  $159.22\text{ J/g}$ . The thermal curve of C-CMTKP showed two endothermic peaks at  $148.55^\circ\text{C}$  and  $214.45^\circ\text{C}$ , with heat flow values of  $524.59\text{ J/g}$  and  $26.997\text{ J/g}$ , respectively.

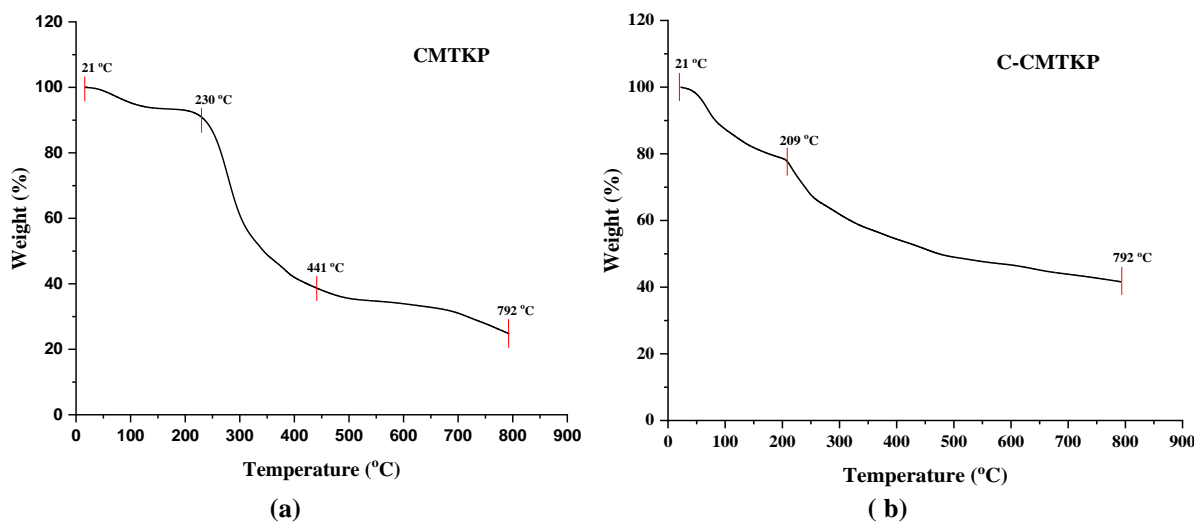


**(a)**



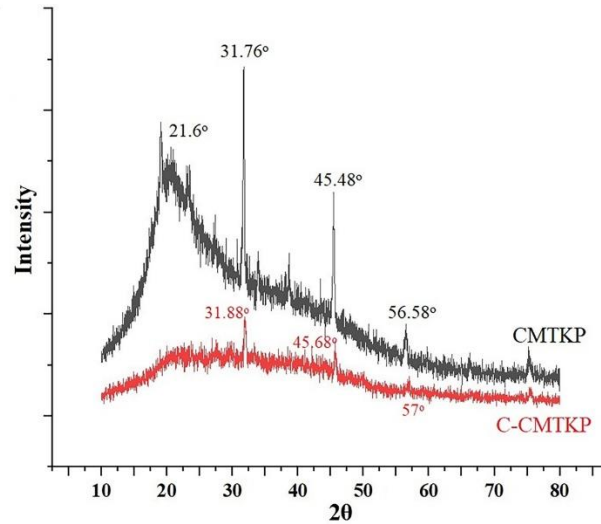
(b)  
**Figure 3.** DSC of CMTKP (a) and C-CMTKP (b).

The C-CMTKP was believed to have more thermal stability than the CMTKP. Therefore, comparative thermal studies were carried out to verify the same. TGA thermograms of CMTKP and C-CMTKP were presented in figure 4 (a) & (b), respectively. The TGA thermogram of CMTKP shows three different stages of weight loss. The polymer's moisture elimination is responsible for the 9.17% weight loss at the beginning stages (21–230°C). The second stage of weight loss (231–441°C) might be due to the deterioration of the polymeric backbone, i.e., the breakdown of hydroxyl & carboxymethyl groups of CMTKP with 52.03% weight loss (Pal et al. 2008). This had been followed by the third stage of deterioration (442–792°C) with a 13.78% weight loss. However, the degradation of C-CMTKP can be seen in two stages on the TGA thermogram. The first stage begins at 21°C & finishes at 209°C, with a 22.41% weight loss. A weight loss of 11.21% was detected in the second stage of deterioration, which began at 210°C and ended at 792°C. Compared to the CMTKP, the C-CMTKP shows more than 41% remaining mass, whereas the CMTKP shows 25% residual mass. As a result, the thermal stability of C-CMTKP was confirmed to be significantly higher than CMTKP.

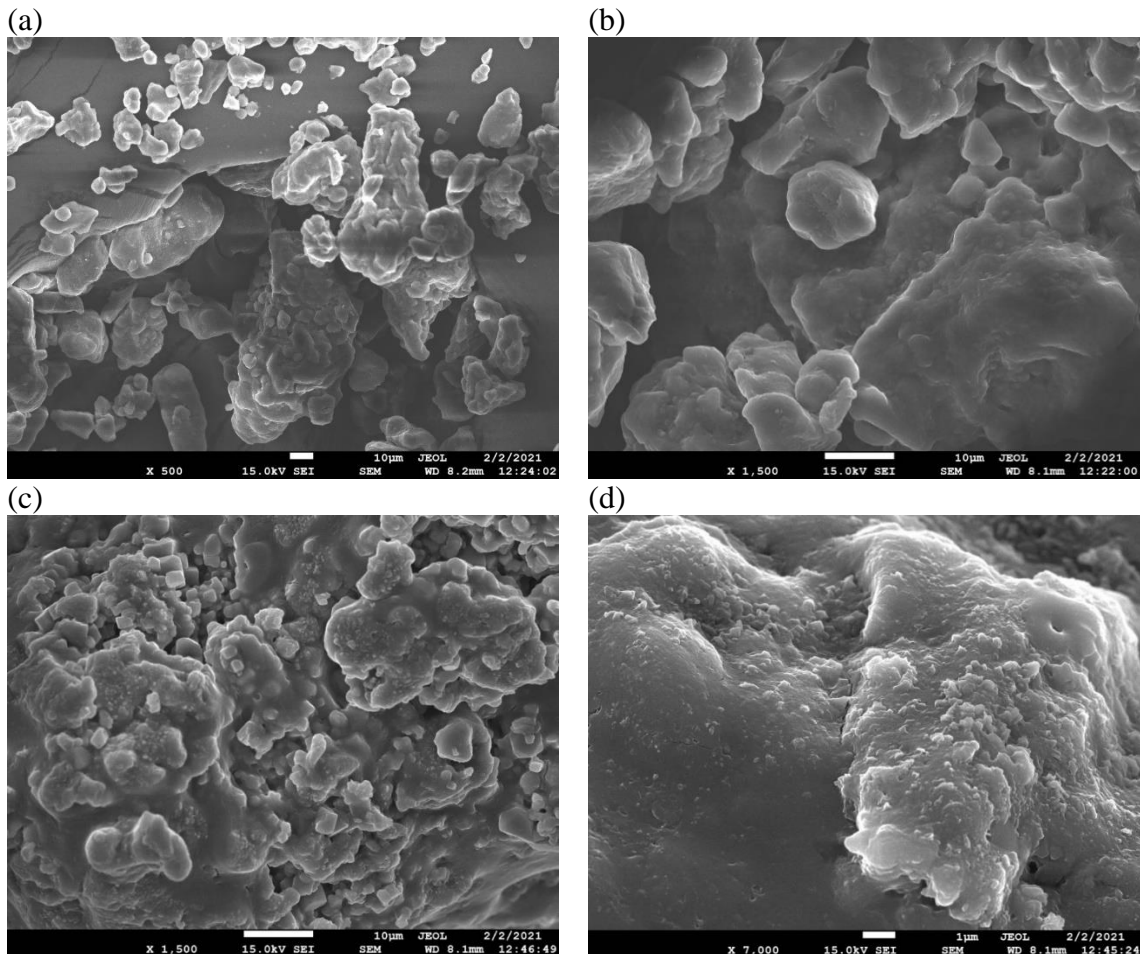


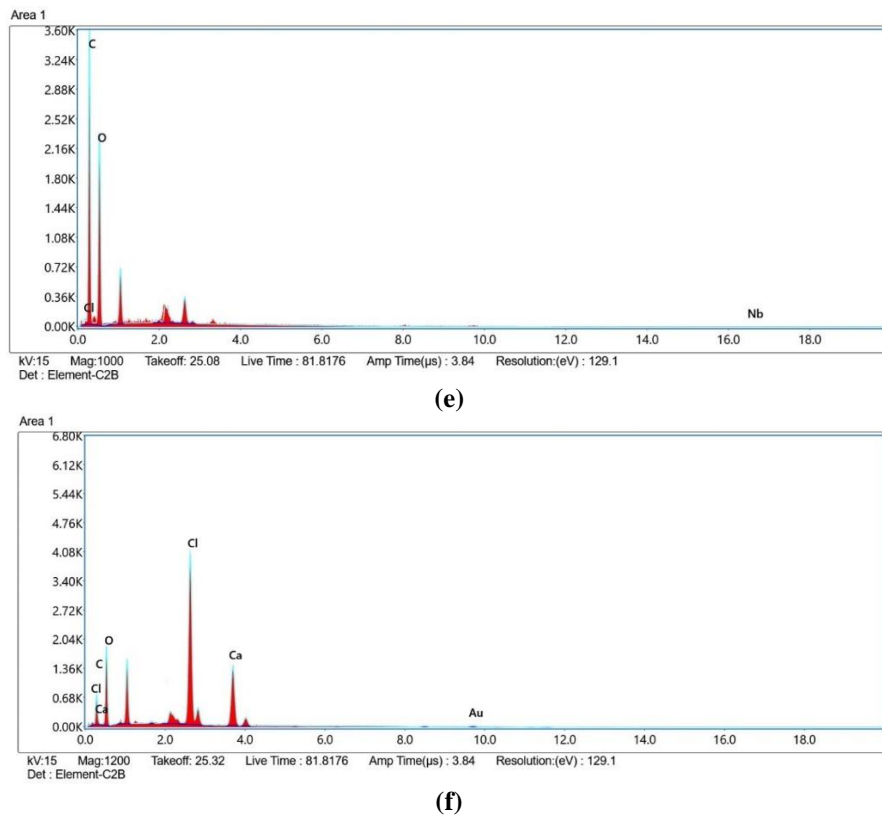
**Figure 4.** TGA of CMTKP (a) and C-CMTKP (b).

Figure 5 compares the X-ray diffraction pattern of CMTKP and C-CMTKP. The X-ray diffraction pattern of CMTKP powder shows the semi-crystalline nature having a diffuse pattern with sharp peaks appearing at 21.6°, 31.76°, 45.48°, and 56.58° (2θ). While the diffraction pattern of C-CMTKP powder shows a diffractogram peak at 31.88°, 45.68°, 57° (2θ) but with reduced intensity. Thus, the study indicates that cross-linking of CMTKP with Ca<sup>2+</sup> diminishes the crystallinity degree.



**Figure 5.** X-ray diffraction of CMTKP and C-CMTKP.





**Figure 6.** Shape (a, c), surface (b, d), and EDX (e, f) spectra of CMTKP and C-CMTKP, respectively.

Figure 6 (a) and (b) shows the shape and surface of CMTKP, and figure 6 (c) and (d) shows the shape and surface of C-CMTKP. The scanning electron micrographic images of CMTKP revealed that carboxymethyl derivatized tamarind gum has a polyhedral shape and a granular surface. In contrast, the microscopical image of C-CMTKP shows that calcium is cross-linked to carboxymethylated gum, having more granules on the surface. Figure 5 (e) and (f) show the EDX spectrum of CMTKP and C-CMTKP, respectively. The EDX spectrum confirms the successful calcium cross-linking of CMTKP gum as the spectrum of C-CMTKP shows an additional calcium peak.

The diclofenac sodium-loaded matrix tablets of CMTKP and C-CMTKP were prepared and comparatively evaluated for their drug delivery applications. The physical characteristics of matrix tablets of diclofenac sodium are shown in table 3.

**Table 3.** Evaluation of matrix tablet.

Parameters	CMTKP	C-CMTKP
Average weight (mg)	403.8 ± 3.85	403.8 ± 2.74
Thickness (mm)	3.95 ± 0.005	3.01 ± 0.01
Diameter (mm)	8.00 ± 0.01	8.00 ± 0.01
Hardness (kg/cm <sup>2</sup> )	4.77 ± 0.54	5.68 ± 0.48
Friability (%)	0.79	0.31
Moisture content (%)	7.10	9.36
Drug content (%)	98.7	98.8

Various tests were done on both batches of CMTKP and C-CMTKP tablets. The average weight of CMTKP(403.8±3.85 mg) and C-CMTKP (403.8±2.74 mg) was found to lie within the percentage of weight variation limits (±5%) as prescribed by the Indian pharmacopeia. The thickness and diameter of the tablet of both the batches of CMTKP and C-CMTKP were observed to be in the range. The thickness of CMTKP and C-CMTKP tablets was found to be 3.95±0.005 mm and 3.01±0.01 mm, respectively. On the other hand, the

diameter was found to be  $8.00 \pm 0.01$  mm for both CMTKP and C-CMTKP. The hardness of CMTKP tablet was found to be  $4.77 \pm 0.54$  kg/cm<sup>2</sup> and the hardness for C-CMTKP was found to be  $5.68 \pm 0.48$  kg/cm<sup>2</sup>. The hardness of both tablets was found in the limit, and thus the tablets passed the hardness test. The friability of tablets was seen to be 0.79% and 0.31% for CMTKP and C-CMTKP, respectively. It shows that this test has passed the result as it was within the pharmacopeia limit, i.e., less than 1%. The results for hardness and friability of C-CMTKP were acceptable for sustained release formulations. It also demonstrated great mechanical strength to withstand physical and mechanical pressure conditions while preserving the integrity of the product.

The moisture content in CMTKP tablet was observed to be 7.10%, while, in C-CMTKP tablet, it was observed to be 9.36%. It can be estimated that the presence of CaCl<sub>2</sub> in C-CMTKP tablets increases the moisture content as found in CMTKP tablets. The total amount of diclofenac drug present in CMTKP tablets was found to be 98.7%, whereas drug content in C-CMTKP tablets was found to be 98.8%.

The *in vitro* release profile of diclofenac sodium from the diclofenac sodium loaded CMTKP and C-CMTKP matrix tablet is shown in figure 7. The experiment was conducted in 0.1N HCl (pH 1.2) for the first 2 h, then in phosphate buffer (pH 6.8) for the next 24 h. The released data shows that 5.62% of the diclofenac sodium was released from the CMTKP tablets, while 4.44 % of the drug was released from the C-CMTKP matrix tablet in 0.1N HCl solution in the first 2 h. On the other hand, 80.6 % and 50.84 % of diclofenac were observed to be released in phosphate buffer solution for the next 24 h. The results indicate that only a small amount of diclofenac is released at pH 1.2; this can be due to the poor solubility of diclofenac at low pH and the protection afforded by the CMTKP and C-CMTKP matrix against erosion at gastric pH. However, the matrix tablets of CMTKP and C-CMTKP start eroding in simulated intestinal fluid, and the drug begins to release. The CMTKP matrix tablets released 80.6 % of diclofenac sodium, while the C-CMTKP matrix tablets were able to sustain the release of diclofenac sodium, giving 50.84 % release over the 24 h.

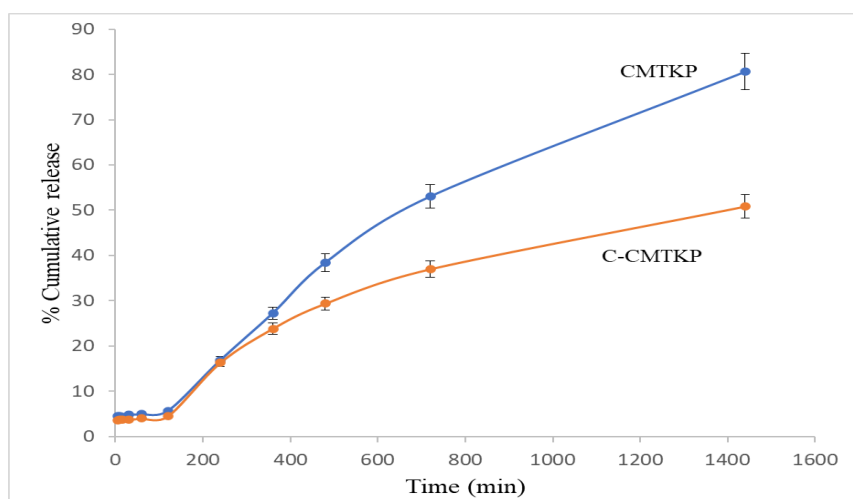


**Figure 7.** The drug release profile of diclofenac sodium tablet composed of CMTKP and C-CMTKP.

The release experiment data was also tested into multiple kinetic models to understand better the release mechanism of diclofenac sodium from matrix tablets. The R<sup>2</sup> values were observed after adjusting the kinetic model data into various models. The R<sup>2</sup> values for CMTKP were found to be 0.9714, 0.9892, 0.9406, and 0.8336 for zero-order, first-order, Higuchi-square root, and Korsmeyer-Peppas models, respectively. The R<sup>2</sup> values for release rate kinetics from

C-CMTKP tablets were 0.9238, 0.9646, 0.9604, and 0.8393 for zero-order, first-order, Higuchi-square root, and Korsmeyer-Peppas models, respectively, as shown in table 4. As a result, the release of diclofenac sodium from the CMTKP and C-CMTKP matrix tablet follows the first-order kinetics. Furthermore, the obtained release exponent ( $n$ ) value for Korsmeyer-Peppas model was 1.5034 for CMTKP and 1.577 for C-CMTKP [33], indicating that the diclofenac sodium release mechanism out of the tablet follows super case – II transport [

**Table 4.** Data from kinetic modeling of drug release.

Batch	R <sup>2</sup> value				
	Zero-order	First order	Higuchi	Korsmeyer-Peppas	
				R <sup>2</sup>	n
CMTKP	0.9714	0.9892	0.9406	0.8336	1.5034
C-CMTKP	0.9238	0.9646	0.9604	0.8393	1.577

#### 4. Conclusions

The carboxymethyl tamarind kernel polysaccharide was successfully cross-linked by reaction with calcium chloride. FT-IR, DSC, TGA, XRD, and FESEM-EDX studies were used to examine the modified carboxymethyl tamarind kernel polysaccharide. XRD study revealed that cross-linked C-CMTKP gum shows amorphous nature with a low degree of crystallinity. Modification of gum was confirmed by FE-SEM and EDX analysis. By formulating diclofenac sodium-loaded tablets, the calcium cross-linked carboxymethyl tamarind kernel polysaccharide was further investigated for pharmaceutical applications. According to *in vitro* release studies, carboxymethyl tamarind kernel polysaccharide calcium cross-linking imparts sustained-release characteristics. As a result, calcium cross-linking of carboxymethyl tamarind kernel polysaccharide appears to be a viable method for improving the release retardant property of the polysaccharide. The drug release was found to follow first-order kinetics with a super case – II transport mechanism of release.

#### Funding

This research received no external funding.

#### Acknowledgments

The author expresses gratitude to Coordinator, DST-FIST, Dept. Of Physics, Guru Jambhsewar University of Science & Technology, Hisar (SR/FST/TSI-089/2005), CSIR-NISCAIR, and AIIMS, New Delhi, for the facility of X-ray diffraction, authentication, and TEM, respectively.

#### Conflicts of Interest

The authors declare no conflict of interest.

#### References

1. Kumar, D.; Mundlia, J.; Kumar, T.; Ahuja, M. Silica coating of carboxymethyl tamarind kernel polysaccharide beads to modify the release characteristics. *International Journal of Biological Macromolecules* **2020**, *146*, 1040–1049, <http://dx.doi.org/10.1016/j.ijbiomac.2019.09.229>.
2. Verma, S.; Rimpay; Ahuja, M. Carboxymethyl modification of *Cassia obtusifolia* galactomannan and its evaluation as sustained release carrier. *International Journal of Biological Macromolecules* **2020**, *164*, 3823-3834, <https://doi.org/10.1016/j.ijbiomac.2020.08.231>.

3. Rimpay, Abhishek; Ahuja, M. Evaluation of carboxymethyl moringa gum as nanometric carrier. *Carbohydrate Polymers* **2017**, *174*, 896–903, <http://dx.doi.org/10.1016/j.carbpol.2017.07.022>.
4. Patra, S.; Bala, N. N.; Nandi, G. Synthesis, characterization and fabrication of sodium carboxymethyl-okragum-grafted-polymethacrylamide into sustained release tablet matrix. *International Journal of Biological Macromolecules* **2020**, *164*, 3885–3900, <http://dx.doi.org/10.1016/j.ijbiomac.2020.09.025>.
5. Sharma, R.; Pahwa, R.; Ahuja, M. Iodine-loaded poly(silicic acid) gellan nanocomposite mucoadhesive film for antibacterial application. *Journal of Applied Polymer Science* **2020**, 1-13, <https://doi.org/10.1002/app.49679>.
6. Meenakshi; Ahuja, M. Metronidazole loaded carboxymethyl tamarind kernel polysaccharide-polyvinyl alcohol cryogels: Preparation and characterization. *International Journal of Biological Macromolecules* **2015**, *72*, 931–938, <https://doi.org/10.1016/j.ijbiomac.2014.09.040>.
7. Makhado, E.; Pandey, S.; Nomngongo, P. N.; Ramontja, J. Preparation and characterization of xanthan gum-cl-poly(acrylic acid)/o-MWCNTs hydrogel nanocomposite as highly effective re-usable adsorbent for removal of methylene blue from aqueous solutions. *Journal of Colloid and Interface Science* **2018a**, *513*, 700–714, <https://doi.org/10.1016/j.jcis.2017.11.060>.
8. Makhado, E., Pandey, S.; Ramontja, J. Microwave assisted synthesis of xanthan gum-cl-poly (acrylic acid) based-reduced graphene oxide hydrogel composite for adsorption of methylene blue and methyl violet from aqueous solution. *International Journal of Biological Macromolecules* **2018b**, *119*, 255–269, <https://doi.org/10.1016/j.ijbiomac.2018.07.104>.
9. Banegas, R.S., Zornio, C.F.; De Borges, A.M.G.; Porto, L.C.; Soldi, V. Preparation, characterization and properties of films obtained from cross-linked guar gum. *Polimeros* **2013**, *23*, 182–188, <http://dx.doi.org/10.4322/polimeros.2013.082>.
10. Bhattacharya, A.; Misra, B.N. Grafting: A versatile means to modify polymers: Techniques, factors and applications. *Progress in Polymer Science* **2004**, *29*, 767–814, <https://doi.org/10.1016/j.progpolymsci.2004.05.002>.
11. Sharma, M.; Rimpay, Verma, S.; Kumar, T.; Ahuja, M. Investigation on microwave-assisted synthesis of carboxymethyl Cassia gum. *Biointerface Research in Applied Chemistry* **2020**, *10*, 6226-6235, <https://doi.org/10.33263/BRIAC105.62266235>.
12. Sharma, R.; Ahuja, M. Thiolated pectin: Synthesis, characterization and evaluation as a mucoadhesive polymer. *Carbohydrate Polymers* **2011**, *85*, 658–663, <https://doi.org/10.1016/j.carbpol.2011.03.034>.
13. Kaur, H.; Ahuja, M.; Kumar, S.; Dilbaghi, N. Carboxymethyl tamarind kernel polysaccharide nanoparticles for ophthalmic drug delivery. *International Journal of Biological Macromolecules* **2012a**, *50*, 833–839, <https://doi.org/10.1016/j.ijbiomac.2011.11.017>.
14. Trivedi, J.H.; Joshi, H.A.; Trivedi, H.C. Synthesis and characterization of photo-graft copolymers of sodium salt of partially carboxymethylated tamarind kernel powder. *Macromolecular Symposia* **2021**, *398*, 1-13, <https://doi.org/10.1002/masy.202000014>.
15. Goyal, P.; Kumar, V.; Sharma, P. Carboxymethylation of tamarind kernel powder. *Carbohydrate Polymers* **2007**, *69*, 251–255, <http://dx.doi.org/10.1016/j.carbpol.2006.10.001>.
16. Kaur, H.; Yadav, S.; Ahuja, M.; Dilbaghi, N. Synthesis, characterization and evaluation of thiolated tamarind seed polysaccharide as a mucoadhesive polymer. *Carbohydrate Polymers* **2012b**, *90*, 1543–1549, <https://doi.org/10.1016/j.carbpol.2012.07.028>.
17. Khushbu; Warkar, S. G.; Thombare, N. Controlled release and release kinetic studies of boron through the functional formulation of carboxymethyl tamarind kernel-gum based superabsorbent hydrogel. *Polymer Bulletin* **2021a**, 1-17, <https://doi.org/10.1007/s00289-021-03634-9>.
18. Jana, S.; Saha, A.; Kumar, A.; Kumar, K.; Kumar, S. Aceclofenac-loaded chitosan-tamarind seed polysaccharide interpenetrating polymeric network microparticles. *Colloids Surf B: Biointerfaces* **2013**, *105*, 303–309, <https://doi.org/10.1016/j.colsurfb.2013.01.013>.
19. Prajapati, V.D.; Mashru, K.H.; Solanki, H.K.; Jani, G.K. Development of modified release gliclazide biological macromolecules using natural biodegradable polymers. *International Journal of Biological Macromolecules* **2013**, *55*, 6–14, <https://doi.org/10.1016/j.ijbiomac.2012.12.033>.
20. Hemalatha, C.; Parameshwari, S. The scope of tamarind (*Tamarindus indica L.*) kernel powder in diverse spheres: A review. *Materials Today: Proceedings* **2021**, *45*, 8144-8148, <https://doi.org/10.1016/j.matpr.2021.02.119>.
21. Ahuja, M.; Kumar, S.; Kumar, A. Tamarind seed polysaccharide-g-poly(n-vinyl-2-pyrrolidone): Microwave-assisted synthesis, characterization, and evaluation as mucoadhesive polymer. *International Journal of Polymeric Materials* **2013**, *62*, 544–549, <http://dx.doi.org/10.1080/00914037.2012.761624>.
22. Khushbu; Warkar, S.W.; Thombare, N. Zinc micronutrient-loaded tamarind kernel gum-based superabsorbent hydrogels: Controlled release and kinetics studies for agricultural applications. *Colloid and Polymer Science* **2021**, *299*, 1103-1111, <https://doi.org/10.1007/s00396-021-04831-8>.
23. Kaur, G.; Jain, S.; Tiwary, A.K. Chitosan-carboxymethyl tamarind kernel powder interpolymer complexation: investigations for colon drug delivery. *Scientia Pharmaceutica* **2010**, *78*, 57–78, <https://doi.org/10.3797/scipharm.0908-10>.

24. Zhang, J.; Xu, S.; Zhang, S.; Du, Z. Preparation and characterization of tamarind gum/sodium alginate composite gel beads. *Iranian Polymer Journal* **2008**, *17*, 899–906.
25. Jana, S.; Banerjee, A.; Sen, K.K.; Maiti, S. Gelatin-carboxymethyl tamarind gum biocomposites: In vitro characterization & anti-inflammatory pharmacodynamics. *Materials Science & Engineering C, Materials for Biological Applications* **2016**, *69*, 478–485, <https://doi.org/10.1016/j.msec.2016.07.008>.
26. Caldwell, J.R. Efficacy and safety of diclofenac sodium in rheumatoid arthritis experience in the United States. *The American Journal of Medicine* **1986**, *80*, 43–47, [https://doi.org/10.1016/0002-9343\(86\)90079-3](https://doi.org/10.1016/0002-9343(86)90079-3).
27. Türker, S.; Erdoğan, S.; Özer, Y.; Bilgili, H.; Deveci, S. Enhanced efficacy of diclofenac sodium-loaded lipogelosome formulation in intra-articular treatment of rheumatoid arthritis. *Journal of Drug Targeting* **2008**, *16*, 51–57, <https://doi.org/10.1080/10611860701725191>,
28. Banihani, S.A. Effect of diclofenac on semen quality: A review. *First International Journal of Andrology Andrologia* **2021**, *53*, 1-7, <https://doi.org/10.1111/and.14021>.
29. Savaşer, A.; Özkan, Y.; İşimer, A. Preparation and *in vitro* evaluation of sustained release tablet formulations of diclofenac sodium. *Farmaco (Societa chimica italiana: 1989)* **2005**, *60*, 171–177, <https://doi.org/10.1016/j.farmac.2004.10.001>.
30. Sujja-Areevath, J.; Munday, D.L.P.J.C.; Khan, K.A. Release characteristics of diclofenac sodium from encapsulated natural gum mini-matrix formulations. *International Journal of Pharmaceutics* **1996**, *139*, 53–62, [https://doi.org/10.1016/0378-5173\(96\)04573-5](https://doi.org/10.1016/0378-5173(96)04573-5).
31. Samaha, D.; Shehayeb, R.; Kyriacos, S. Modeling and comparison of dissolution profiles of diltiazem modified-release formulations. *Dissolution Technologies* **2009**, *16*, 41–46, <https://doi.org/10.14227/DT160209P41>.
32. Bachra, Y.; Grouli, A.; Damiri, F.; Talbi, M.; Berrada, M. A novel superabsorbent polymer from crosslinked-carboxymethyl tragacanth gum with glutaraldehyde: Synthesis, characterization and swelling properties. *International Journal of Biomaterials* **2021**, *2021*, 1-14, <https://doi.org/10.1155/2021/5008833>.
33. Barmpalexis, P.; Kachrimanis, K.; Malamataris, S. Statistical moments in modelling of swelling, erosion and drug release of hydrophilic matrix-tablets. *International Journal of Pharmaceutics* **2018**, *540*, 1–10, <https://doi.org/10.1016/j.ijpharm.2018.01.052>.